ADVANCED FUNCTIONAL MATERIALS
www.afm-journal.de



# Fabrication of Organic Thin-Film Transistors on Three-Dimensional Substrates Using Free-Standing Polymeric Masks Based on Soft Lithography

*Ju-Hyung Kim, Sang Ho Hong, Kwang-dong Seong, and Soonmin Seo**

**Here, a novel fabrication technique for integrated organic devices on substrates with complex structure is presented. For this work, free-standing polymeric masks with stencil-patterns are fabricated using an ultra-violet (UV) curable polyurethaneacrylate (PUA) mixture, and used as shadow masks for thermal evaporation. High flexibility and adhesive properties of the free-standing PUA masks ensure conformal contact with various materials such as glass, silicon (Si), and polymer, and thus can also be utilized as patterning masks for solution-based deposition methods, such as spin-coating and drop-casting. Based on this technique, a number of integrated organic transistors are fabricated simultaneously on a cylindrical glass bottle with high curvature, as well as on a flat silicon wafer. It is anticipated that these results will be applied to the development of various integrated organic devices on complex-structured substrates, which can lead to further applications.**

## 1. Introduction

Extensive research has been carried out on the practical applications of organic electronics, such as organic light-emitting diodes (OLEDs),[1,2] organic thin-film transistors (OTFTs),[3–5] and organic photovoltaics (OPVs),[6,7] due to their outstanding advantages compared to standard inorganic technologies.[8,9] The performance of organic devices has been enhanced dramatically by the research efforts ranging from molecular design to device-fabrication methods,[10–14] some of which have already been commercialized in current electrical appliances. New functionalities that can be introduced to organic devices, such as flexibility,[15–17] wearability,[18] and patchability,[19] are also receiving much attention for further applications.

Fabrication techniques for organic devices, including flexible, wearable, or patchable devices, have advanced rapidly, but they are normally fabricated on flat substrates. Electrode layers in organic devices are mostly deposited by a thermal evaporation process though a rigid shadow mask, and the conventional shadow masking process hinders the production of uniform electrode layers on complex-structured substrates such as bottle-shaped substrates. In case of soft materials for alternative shadow masks, such as polymers and adhesive tapes, there has been trouble with realizing minute patterns on shadow masks, which are necessary for fabricating integrated devices as well.[20–23] Thus, a fresh technique is required to fabricate organic devices on complex-structured substrates for further applications, such as highly integrated devices with small area, or smart glasses with high curvature.[24,25]

We present a novel fabrication technique for integrated organic devices on complex-structured substrates. For this work, we have used free-standing polymeric stencils as shadow masks with high flexibility and adhesive properties, which enable conformal contact with various materials such as glass, silicon (Si), and polymer.[26–30] This technique based on soft lithography facilitates the patterning of polymeric stencils on the scale of a few μm ranges, and also can be easily utilized to fabricate free-standing shadow masks not only for thermal evaporation but also for solution-based deposition methods, such as spin-coating and drop-casting.[31–34] We demonstrate direct fabrication processes of integrated OTFTs on a cylindrical glass bottle in addition to a flat Si wafer using this technique. The results strongly suggest potential for the development of various integrated organic devices on complex-structured substrates which can lead to their new applications.

## 2. Results and Discussion

The free-standing polymeric stencils used in this work were prepared as schematically illustrated in **Figure 1**. An ultra-violet (UV) curable polyurethaneacrylate (PUA) mixture was drop-dispensed onto a master-pattern of polydimethylsiloxane (PDMS) mold, and then covered with another flat PDMS mold.[35] Due to the properties of conformal contact between the two PDMS molds and the high UV transparency of PDMS, a PUA replica with the stencil-pattern (i.e., negative empty space of the master-pattern, as illustrated in Figure 1) could be easily prepared after the UV curing and peeling off the PDMS molds (see

Dr. J.-H. Kim
BioNano Sensor Research Center
Gachon University
Gyeonggi, 461–701, Republic of Korea
S. H. Hong, K.-d. Seong, Prof. S. Seo
College of BioNano Technology
Gachon University
Gyeonggi, 461–701, Republic of Korea
E-mail: soonmseo@gachon.ac.kr

DOI: 10.1002/adfm.201303478

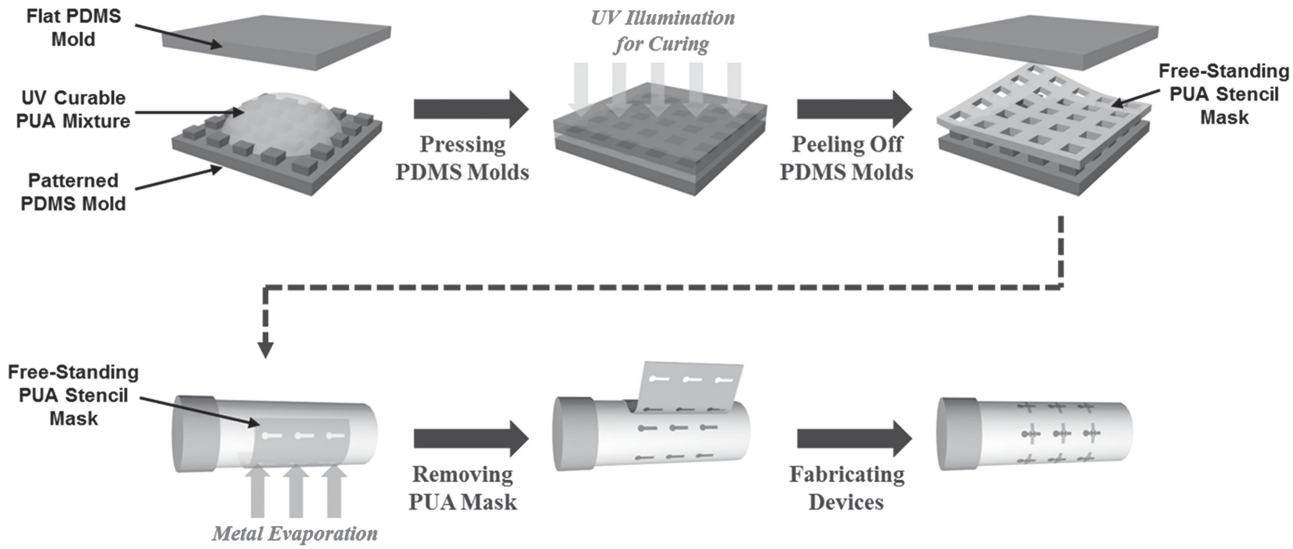


**Figure 1.** Schematic illustration of preparation and use of a free-standing PUA mask. Since a drop-dispensed UV curable PUA mixture fills the empty space between the two PDMS molds, a free-standing PUA replica with a stencil-pattern is easily prepared after UV curing, which can be utilized as a shadow mask for various film-deposition methods, such as thermal evaporation.

Experimental Section). To avoid deformations of the master-pattern of the PDMS mold such as pairing and sagging in this procedure, the aspect ratio (i.e., the ratio of the height to the width) of the master-pattern should be in the range between 0.2 and 2.[31,36] In addition, the height of the mater-pattern is critical in fabrication of the stencil-pattern, because the absence of residual PUA layer within the contact area of the two PDMS molds is necessary for the stencil-pattern. Thus, there are difficulties in realizing the PUA replica with the stencil-pattern on a sub-micrometer scale without applying high pressure (>2 MPa). This PUA replica with the stencil-pattern can be used as a free-standing shadow mask with high flexibility and adhesive properties as shown in **Figure 2**, and its stencil-pattern is easily tunable within a few μm by the master-pattern of the PDMS mold (Figure 2d). Note that the properties of the PUA replica which can be soft or hard are controllable by modulating the materials contained in the PUA mixture.[35] Since a soft PUA replica with high flexibility and adhesive properties ensures conformal contact with complex-structured substrates, only the soft PUA material was used in this work. It has been well-known that the soft PUA material has a tensile modulus of ≈19.8 MPa, and elongation at break of 45%.[35] Remaining unsaturated acrylate in the soft PUA material after the UV curing provides adhesive properties in addition to such high flexibility.[37]

To investigate the properties of the contact between the free-standing polymeric stencil and the substrate, 5 wt% of poly(methylmethacrylate) (PMMA) in toluene was spin-coated onto the PUA mask with the stencil-pattern in contact with the Si wafer. Each motif of the PUA stencil-pattern was a square shape with a length and width of 1500 μm, and a thickness of 100 μm. After peeling off the PUA mask from the substrate, the spin-coated PMMA layer was examined by scanning electron microscopy (SEM), as shown in **Figure 3**. Since the PMMA solution cannot penetrate into the contact region between the PUA mask and the substrate, the PMMA was coated only along the side walls and bottom of the PUA stencil-pattern (Figure 3a). This result indicates that the PUA mask and the substrate tightly stick to each other without any external forces applied, and form conformal contact between

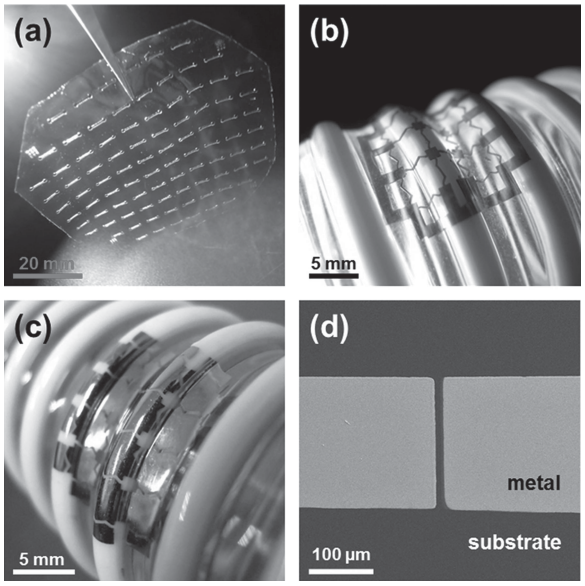


**Figure 2.** a) Photo image of the free-standing PUA mask with the stencil-pattern (10 cm × 10 cm), which was prepared as illustrated in Figure 1. b) Photo image of the free-standing PUA mask attached to the complex-structured substrate, which shows high flexibility and adhesive properties. c) Photo image of the Au electrodes on the complex-structured substrate deposited by thermal evaporation through the free-standing PUA masks. d) SEM image of the deposited Au electrodes on the Si wafer prepared as illustrated in Figure 1. Spacing between the electrodes is tunable corresponding to the master-pattern of PDMS mold within a few μm ranges. The distance between the two electrodes in (d) is 10 μm, and the scale bar represents 100 μm.

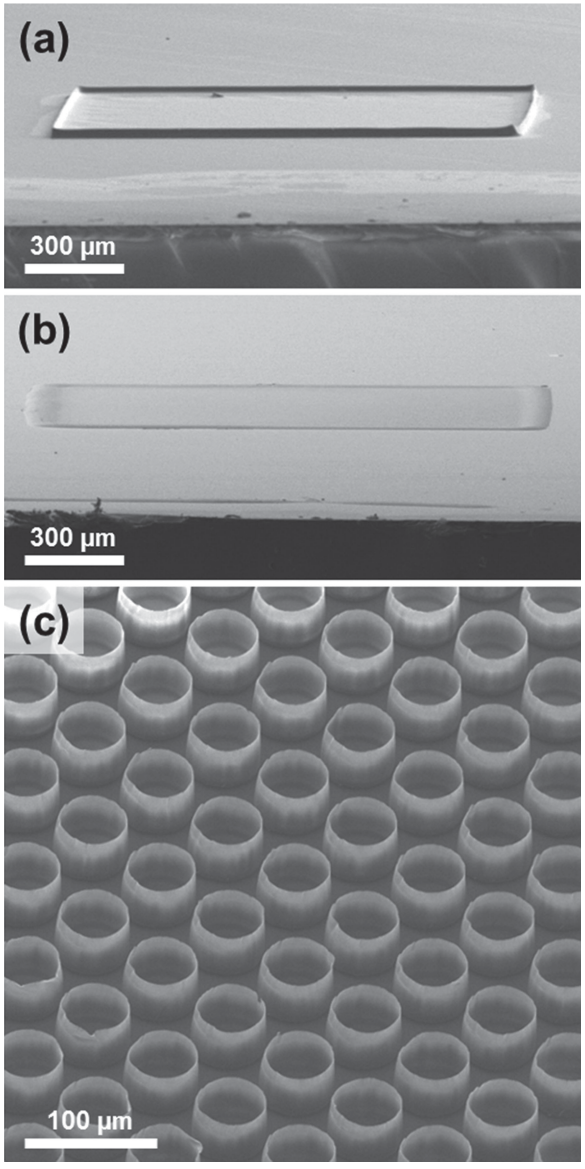


**Figure 3.** a) SEM image of the PMMA layer which was spin-coated onto the PUA mask with the stencil-pattern in contact with the Si wafer. Each motif of the PUA stencil-pattern was a square shape with a length and width of 1500 μm, and a thickness of 100 μm. PMMA is coated only along the side walls and bottom of the stencil-pattern, because the PMMA solution cannot penetrate into the contact region between the PUA mask and substrate. The scale bar represents 300 μm. b) SEM image of the spin-coated PMMA layer after thermal annealing. When the spin-coated PMMA pattern is thermally annealed at a higher temperature (≈180 °C) than the glass transition temperature of PMMA (≈105 °C), the side walls of the PMMA pattern are collapsed and flattened with an average thickness of 400–500 nm. c) SEM image of an exemplary PMMA pattern prepared by one-step spin-coating. The radius of each motif was 25 μm, and a uniform pattern of PMMA was easily achieved on a relatively large area (3 cm × 3 cm).

them. Due to a relatively short time of the spin-coating process (30 s) and no penetration of the PMMA solution into the contact region, any effect of solvent swelling was not observed in this procedure. It is worth noting that the soft PUA material used in this work shows only small effect of solvent swelling when a cured PUA replica was immersed in pure ethanol for 3 h.[35] In addition, when the spin-coated PMMA pattern was thermally annealed at a higher temperature (≈180 °C) than the glass transition temperature of PMMA (≈105 °C), the side walls of the spin-coated PMMA pattern were collapsed and flattened with a thickness of 400–500 nm. The flattened PMMA pattern by the thermal treatment basically conforms to the shape of the original PUA stencil-pattern (Figure 3b), which indicates that the free-standing PUA mask can play a role in fabricating a desired pattern via spin-coating. Figure 3c shows an exemplary PMMA pattern fabricated using the free-standing PUA mask. The radius of each motif was 25 μm, and the uniform pattern of PMMA was easily achieved on a relatively large area (3 cm × 3 cm) by one-step spin-coating.

**Figure 4** shows a demonstration of fabricating the OTFT on the Si wafer using the free-standing PUA masks. The OTFT was constructed with a bottom-gate configuration using aluminum (Al) and gold (Au) electrodes and a pentacene active layer, as illustrated in Figure 4a. The channel length and width between the Au source and drain electrodes were 100 μm

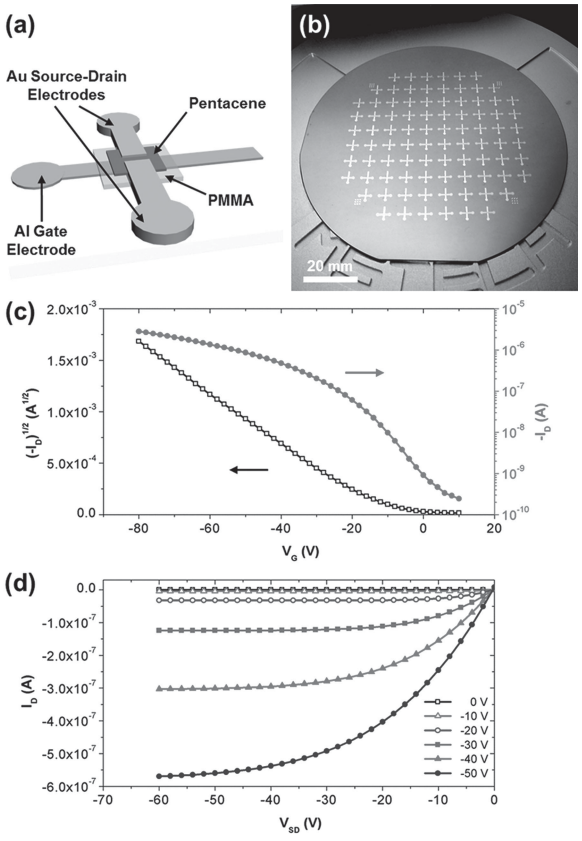


**Figure 4.** a) Schematic illustration of the OTFT structure constructed with a bottom-gate configuration. b) Photo image of ninety-one exemplary OTFTs simultaneously integrated on a four-inch Si wafer. c) Transfer characteristics of the OTFT fabricated on the Si wafer in log scale (indicated by filled red circles) and in square-root scale (indicated by unfilled black squares). Measurement was performed at a fixed source-drain voltage of –60 V. d) Output characteristics of the same device.

and 500 μm, respectively. For this demonstration, four PUA free-standing masks with different stencil-patterns were individually used to deposit each component of the OTFT with proper shape and alignment, as indicated in Figure 4a. The Al and Au electrodes and the pentacene layer were deposited by thermal evaporation through the PUA masks, and only the PMMA layer was spin-coated and thermally annealed (Figure 3b). Figure 4 also shows the field-effect transistor (FET) characteristics of the fabricated OTFT with gate modulation. An average hole mobility of ≈0.12 $cm^2 V^{-1} s^{-1}$ in the saturation regime, an on-to-off current ratio of ≈$3 \times 10^3$, and a threshold voltage of ≈2.0 V were achieved. This fabrication technique can be easily applied to large-area electronics, because the free-standing PUA mask guarantees conformal contact regardless of the size of the substrate. Figure 4b shows ninety-one exemplary OTFTs which were simultaneously integrated on a four-inch Si wafer. For this demonstration, each PUA free-standing mask was aligned onto the Si wafer substrate before peeling off the PDMS mold with the master-pattern from the cured PUA mask. Since both PDMS and PUA materials are transparent, an accurate alignment of the mask onto the substrate was easily achieved using an optical microscope. The dimension of each OTFT was 5 mm × 5 mm, and the center-to-center distance between the OTFTs was 7 mm in both row and column directions.

After obtaining the FET characteristics on the flat Si wafer, the integrated OTFTs were directly fabricated on a cylindrical glass bottle to examine the possibility of fabricating organic devices on complex-structured substrates using the free-standing PUA masks, as shown in **Figure 5**. Eighteen OTFTs in total were simultaneously fabricated on a cylindrical glass bottle with a radius of 12.5 mm and length of 62 mm, and each OTFT was constructed in the same configuration as in Figure 4a. Since a spin-coating process is not feasible for a highly curved substrate, the 1.5 wt% PMMA solution was drop-dispensed onto the patterned PUA mask that was in contact with the bottle substrate and then thermally annealed at a higher temperature (≈180 °C) than the glass transition temperature of PMMA (≈105 °C) to prepare the insulating layers in the integrated OTFTs. In addition, to preserve the uniformity of the deposited Al and Au electrodes and the pentacene layers, the bottle substrate was rotated at 12 rpm during the whole thermal evaporation processes. For an alignment of the mask onto the bottle substrate, an arbitrary selected row of the stencil pattern was aligned first using an optical microscope. Then, careful attachment of the remaining part of the mask onto the substrate could lead to a simultaneous alignment of the mask, because the dimension (5 mm × 5 mm for each OTFT) and the center-to-center distance (7 mm between the OTFTs) were identical in each individual PUA mask. Figure 5 also shows the typical FET characteristics of the fabricated devices with gate modulation. An average hole mobility of ≈0.17 $cm^2 V^{-1} s^{-1}$ (range 0.14–0.18 $cm^2 V^{-1} s^{-1}$) in the saturation regime, an on-to-off current ratio of ≈$10^4$, and a threshold voltage of ≈2.0 V were achieved. These results indicate that the free-standing PUA masks can be successfully utilized for various film-deposition methods such as thermal evaporation, spin-coating, and drop-casting, and also enable the fabrication of integrated organic devices directly on complex-structured substrates.

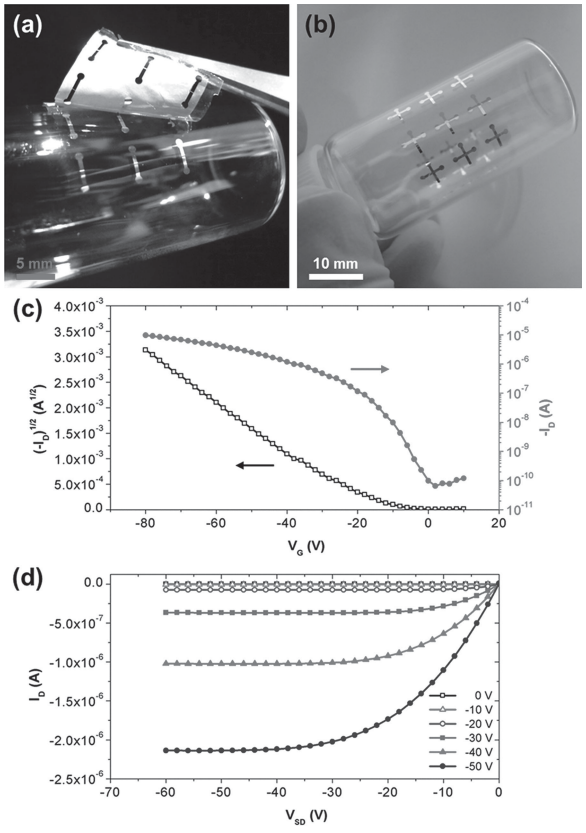


**Figure 5.** a) Photo image of the deposited Al gate electrodes on the cylindrical bottle substrate using the free-standing PUA mask. b) Photo image of the OTFTs integrated on the cylindrical bottle substrate. Eighteen OTFTs in total were simultaneously constructed in the same configuration as in Figure 4a. The radius and length of the cylindrical bottle substrate were 12.5 mm and 62.0 mm, respectively. c) Transfer characteristics of the OTFT fabricated on the cylindrical bottle substrate in log scale (indicated by filled red circles) and in square-root scale (indicated by unfilled black squares). Measurement was performed at a fixed source-drain voltage of –60 V. d) Output characteristics of the same device.

## 3. Conclusions

We have introduced a novel fabrication process for OTFTs integrated on a complex-structured substrate using free-standing polymeric masks with high flexibility and adhesive properties. The free-standing polymeric mask is easily patterned and prepared with a soft PUA mixture, and also enables conformal contact with various materials. Thus, the free-standing polymeric masks can be successfully used as shadow masks for various film-deposition methods, such as thermal evaporation, spin-coating, and drop-casting. As such, the free-standing polymeric masks facilitate the fabrication of organic devices integrated on complex-structured substrates, and shows promise as an easy process for large-area electronics. Based on this technique, a number of integrated OTFTs were simultaneously fabricated on a cylindrical glass bottle with a high curvature, as well as on a flat Si wafer. We anticipate that these results will be applied to the development of various integrated organic devices on complex-structured substrates, which can lead to further applications.

## 4. Experimental Section

*Preparation of a Free-Standing PUA Mask*: A UV curable PUA mixture synthesized in accordance with previous reports was drop-dispensed onto a master-pattern PDMS mold,[35,38] and then covered with another flat PDMS mold. To squeeze out the excess amount of the PUA mixture between the two PDMS molds, pressure was applied from one end of the flat PDMS mold toward the other end using a roller.[39] Due to the properties of conformal contact between the two PDMS molds, the two molds were easily brought into contact with each other after this sequential rolling, and the only empty space between them was filled with the PUA mixture. Then the PUA mixture was exposed to UV light ($\lambda \approx 365$ nm) for several minutes through the UV transparent PDMS molds. After the UV curing, the two PDMS molds were easily peeled off, and a free-standing PUA replica with the stencil-pattern (i.e., negative empty space of the master-pattern of PDMS mold) was prepared.

*Fabrication of OTFTs on the Si Wafer*: The overall structure of OTFTs used in this work had a bottom-gate configuration (Al/PMMA/pentacene/Au). Four PUA free-standing masks with different stencil-patterns were individually prepared to deposit each component of the OTFT with proper shape and alignment. In a vacuum chamber, the Al gate electrode (70 nm) was thermally deposited onto the Si wafer through the PUA mask, which was in contact with the substrate. After replacing the PUA mask, 5 wt% of PMMA in toluene was spin-coated onto the PUA mask in contact with the Al-coated substrate. To flatten the PMMA layer after the spin-coating process, the sample was thermally annealed at ≈180 °C in a vacuum oven for 1 h. During the thermal annealing of the sample, the average thickness of the flattened PMMA layer reached 400–500 nm. Then, the pentacene layer (70 nm) and the Au source and drain electrodes (70 nm) were thermally deposited onto the sample consecutively through the individual free-standing PUA masks. For an alignment of the PUA free-standing mask, each mask was aligned onto the Si wafer substrate before peeling off the PDMS mold with the master-pattern from the cured PUA mask. Since both PDMS mold and PUA mask are transparent, an accurate alignment of the mask onto the Si wafer was achieved using an optical microscope.

*Fabrication of OTFTs on the Cylindrical Bottle Substrate*: The preparation procedure of the OTFTs on the cylindrical bottle substrate is basically the same as on the Si wafer, except for the preparation of the insulating PMMA layer. Since the spin-coating process is not applicable to highly curved substrates, the 1.5 wt% PMMA solution was drop-dispensed (≈0.5 μL) onto the PUA mask in contact with the Al-coated cylindrical substrate, and then thermally annealed at ≈180 °C in a vacuum oven for 1 h. During the thermal annealing of the sample, the average thickness of the PMMA layer reached 500 nm. In addition, to preserve the uniformity of the thermally deposited layers, the bottle substrate was rotated at 12 rpm during the whole thermal evaporation process. For an alignment of the mask onto the cylindrical bottle substrate, an arbitrary selected row of the stencil pattern was aligned first using an optical microscope. Then, a simultaneous alignment of the mask could be achieved by careful attachment of the remaining part of the mask onto the substrate, because the dimension and the center-to-center distance were identical in each individual PUA mask.

## Acknowledgements

J.-H.K., S.H.H., and K.-d.S. contributed equally to this work. This work was supported by the Gachon University research fund of 2014 (GCU-2013-R338).

Received: October 10, 2013
Revised: November 14, 2013
Published online: December 27, 2013

[1] J. Burroughes, D. Bradley, A. Brown, R. Marks, K. Mackay, R. Friend, P. Burns, A. Holmes, *Nature* **1990**, *347*, 539.
[2] M. T. Bernius, M. Inbasekaran, J. O'Brien, W. Wu, *Adv. Mater.* **2000**, *12*, 1737.
[3] C. D. Dimitrakopoulos, P. R. L. Malenfant, *Adv. Mater.* **2002**, *14*, 99.
[4] G. Horowitz, *J. Mater. Res.* **2004**, *19*, 1946.
[5] H. Klauk, *Chem. Soc. Rev.* **2010**, *39*, 2643.
[6] S. Gunes, H. Neugebauer, N. S. Sariciftci, *Chem. Rev.* **2007**, *107*, 1324.
[7] T. Ameri, G. Dennler, C. Lungenschmied, C. J. Brabec, *Energy Environ. Sci.* **2009**, *2*, 347.
[8] S. R. Forrest, *Nature* **2004**, *428*, 911.
[9] H. Ma, H. L. Yip, F. Huang, A. K. Y. Jen, *Adv. Funct. Mater.* **2010**, *20*, 1371.
[10] C. Kim, P. E. Burrows, S. R. Forrest, *Science* **2000**, *288*, 831.
[11] C. R. Newman, C. D. Frisbie, D. A. da Silva Filho, J.-L. Brédas, P. C. Ewbank, K. R. Mann, *Chem. Mater.* **2004**, *16*, 4436.
[12] Y. Shirota, *J. Mater. Chem.* **2004**, *15*, 75.
[13] A. L. Briseno, S. C. Mannsfeld, M. M. Ling, S. Liu, R. J. Tseng, C. Reese, M. E. Roberts, Y. Yang, F. Wudl, Z. Bao, *Nature* **2006**, *444*, 913.
[14] J. F. Chang, H. Sirringhaus, *Adv. Mater.* **2009**, *21*, 2530.
[15] D.-H. Kim, J.-H. Ahn, W. M. Choi, H.-S. Kim, T.-H. Kim, J. Song, Y. Y. Huang, Z. Liu, C. Lu, J. A. Rogers, *Science* **2008**, *320*, 507.
[16] J. A. Rogers, T. Someya, Y. Huang, *Science* **2010**, *327*, 1603.
[17] T. Sekitani, T. Someya, *Adv. Mater.* **2010**, *22*, 2228.
[18] L. Hu, M. Pasta, F. L. Mantia, L. Cui, S. Jeong, H. D. Deshazer, J. W. Choi, S. M. Han, Y. Cui, *Nano Lett.* **2010**, *10*, 708.
[19] D.-H. Kim, N. Lu, R. Ma, Y.-S. Kim, R.-H. Kim, S. Wang, J. Wu, S. M. Won, H. Tao, A. Islam, *Science* **2011**, *333*, 838.
[20] D. C. Duffy, R. J. Jackman, K. M. Vaeth, K. F. Jensen, G. M. Whitesides, *Adv. Mater.* **1999**, *11*, 546.
[21] S. K. Park, D. A. Mourey, S. Subramanian, J. E. Anthony, T. N. Jackson, *Adv. Mater.* **2008**, *20*, 4145.
[22] H.-S. Chuang, S. T. Wereley, *J. Micromech. Microeng.* **2009**, *19*, 097001.
[23] J. K. Wassei, V. C. Tung, S. J. Jonas, K. Cha, B. S. Dunn, Y. Yang, R. B. Kaner, *Adv. Mater.* **2010**, *22*, 897.
[24] H. T. Ng, J. Han, T. Yamada, P. Nguyen, Y. P. Chen, M. Meyyappan, *Nano Lett.* **2004**, *4*, 1247.
[25] J. Goldberger, A. I. Hochbaum, R. Fan, P. Yang, *Nano Lett.* **2006**, *6*, 973.
[26] A. Bietsch, B. Michel, *J. Appl. Phys.* **2000**, *88*, 4310.
[27] Y. S. Kim, H. H. Lee, P. T. Hammond, *Nanotechnology* **2003**, *14*, 1140.
[28] K. Y. Suh, S. J. Choi, S. J. Baek, T. W. Kim, R. Langer, *Adv. Mater.* **2005**, *17*, 560.
[29] R. Pal, K. E. Sung, M. A. Burns, *Langmuir* **2006**, *22*, 5392.
[30] J. K. Hwang, S. Cho, J. M. Dang, E. B. Kwak, K. Song, J. Moon, M. M. Sung, *Nat. Nanotechnol.* **2010**, *5*, 742.
[31] Y. Xia, G. M. Whitesides, *Angew. Chem. Int. Ed.* **1998**, *37*, 550.
[32] D. Suh, S.-J. Choi, H. H. Lee, *Adv. Mater.* **2005**, *17*, 1554.
[33] J. A. Rogers, R. G. Nuzzo, *Mater. Today* **2005**, *8*, 50.
[34] D. Qin, Y. Xia, G. M. Whitesides, *Nat. Protoc.* **2010**, *5*, 501.
[35] P. J. Yoo, S.-J. Choi, J. H. Kim, D. Suh, S. J. Baek, T. W. Kim, H. H. Lee, *Chem. Mater.* **2004**, *16*, 5000.
[36] E. Delamarche, H. Schmid, B. Michel, H. Biebuyck, *Adv. Mater.* **1997**, *9*, 741.
[37] R. Kwak, H. E. Jeong, K. Y. Suh, *Small* **2009**, *5*, 790.
[38] S.-J. Choi, P. J. Yoo, S. J. Baek, T. W. Kim, H. H. Lee, *J. Am. Chem. Soc.* **2004**, *126*, 7744.
[39] S.-J. Choi, D. Tahk, H. Yoon, *J. Colloid Interface Sci.* **2009**, *340*, 74.